

Precise predictions for polarised weak bosons at the LHC

Giovanni Pelliccioli

Max-Planck-Institut für Physik, Föhringer Ring 6, 80805 München, Germany



Precise and accurate Standard Model predictions are needed for polarised weak bosons in LHC processes, in order to perform template fits of data and to enhance the sensitivity to possible new-physics effects. We have proposed a general strategy to compute polarised cross-sections including radiative QCD and electroweak corrections to the production and decay of bosons. The method relies on the pole approximation and the separation of polarisation states at amplitude level. After showing some details of the theoretical definition, we present results relevant for LHC di-boson polarisation analyses in semi-leptonic decay channels.

1 Motivation

The LHC luminosities accumulated in Run 2 and foreseen in next runs (Run 3, High-Lumi) will enable precise measurements of electroweak (EW) processes with one or more weak bosons (W^\pm , Z). Accessing the polarisation state of weak bosons represents a crucial step towards a better understanding of the electroweak-symmetry-breaking mechanism realised in nature, providing us with important probes of the Standard Model (SM) gauge and Higgs sectors, as well as high discrimination power between SM and beyond-the-SM (BSM) dynamics. Unfortunately, extracting EW-boson polarisation states is hampered by the unstable nature of massive gauge bosons, making it impossible to directly detect polarised bosons. However, the polarisation state of W and Z bosons leaves trace in the kinematic distributions of the decay products. The typical approach used in Run-1 polarisation analyses relied on the extraction of coefficients from decay-product angular distributions¹. More recently, a template-fit approach was introduced by ATLAS and CMS in the analysis programme, leading to polarisation measurements in di-boson inclusive production² and scattering³. Sensitivity studies for polarisation measurements in the High-Lumi and High-Energy stages of the LHC are promising⁴. In order to enable fits of LHC data with polarised templates, we need three ingredients from the theory side: (1) proper control on the definition of polarised signals, (2) high accuracy in the perturbative and non-perturbative predictions, and (3) clever ideas to enhance the sensitivity to polarisation in the LHC environment.

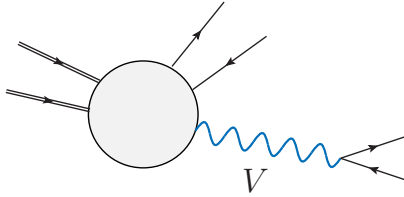


Figure 1 – Generic resonant contribution to single-boson production and decay.

2 Theoretical definition of polarised signals

A natural definition of polarised signals can be identified in the case of processes that are described by resonant diagrams (in a certain on-shell approximation, with a given gauge choice). In the t’Hooft-Feynman gauge, the (unpolarised) amplitude for resonant diagrams as the one in Fig. 1 can be written as,

$$\mathcal{A}^{\text{unp}} = \mathcal{P}_\mu \frac{-g^{\mu\nu}}{k^2 - M_V^2 + iM_V\Gamma_V} \mathcal{D}_\nu = \mathcal{P}_\mu \frac{\sum_{\lambda'} \varepsilon_{\lambda'}^\mu \varepsilon_{\lambda'}^{*\nu}}{k^2 - M_V^2 + iM_V\Gamma_V} \mathcal{D}_\nu. \quad (1)$$

The sum runs over physical polarisation modes as unphysical modes are canceled by Goldstone-boson contributions. Replacing the sum with a single term we obtain a polarised amplitude,

$$\mathcal{A}_\lambda = \mathcal{P}_\mu \frac{\varepsilon_\lambda^\mu \varepsilon_\lambda^{*\nu}}{k^2 - M_V^2 + iM_V\Gamma_V} \mathcal{D}_\nu, \quad \text{for polarisation } \lambda = \text{L}, +, -. \quad (2)$$

Therefore, the squared unpolarised amplitude is written an incoherent sum of squared polarised amplitudes plus interference terms:

$$|\mathcal{A}^{\text{unpol}}|^2 = \sum_\lambda |\mathcal{A}_\lambda|^2 + \sum_{\lambda \neq \lambda'} \mathcal{A}_\lambda^* \mathcal{A}_{\lambda'} \quad (3)$$

Up to flux, symmetry and phase-space factors, we obtain a natural definition of *polarised cross section* proportional to $|\mathcal{A}_\lambda|^2$ ⁶. Note that polarisation vectors (and therefore polarised signals) are defined in a specific Lorentz frame. As mentioned above the decay-product distributions reflect the polarisation state of the decayed boson, thus the polarisation fractions (f_{L}, f_{\pm}) can be extracted from the unpolarised decay-angle distribution⁵,

$$\frac{d\sigma}{d\cos\theta^*} \frac{1}{\sigma} = \frac{3f_{\text{L}}}{4}(1 - \cos^2\theta^*) + \frac{3f_{+}}{8}(1 + \cos^2\theta^* + 2c_{\text{RL}}\cos\theta^*) + \frac{3f_{-}}{8}(1 + \cos^2\theta^* - 2c_{\text{RL}}\cos\theta^*), \quad (4)$$

by means of projections onto suitable spherical harmonics. However, this strategy is not viable with more than one bosons, with radiative corrections modifying the decay structure, and in the presence of cuts on decay products^{5,6}. On the contrary, the polarised-signal definition of Eq. 3 can be systematically applied in the presence of more bosons and including such realistic effects.

Since in general both resonant and non resonant diagrams contribute to any LHC process already at leading order (LO), only resonant diagrams must be selected, recovering the EW gauge invariance by means of a narrow-width or pole approximation⁷. Then, separating polarised amplitudes is straightforward. This strategy can be applied to processes with any number of EW bosons and a general method was proposed^{8,9} to extend it also to the presence of next-to-leading-order (NLO) QCD and EW corrections (both to production and to decay). This has been successfully applied to all di-boson processes in the fully leptonic decay channel up to NNLO QCD and NLO EW accuracy^{8,10,9}. The extension of the method to the NLO matching to parton showers is ongoing in the POWHEG-BOX-RES framework¹¹.

Table 1: Fiducial cross sections and fractions for (un)polarised ZW^+ production with semi-leptonic decays for the two setups. Monte Carlo errors (in parentheses) and QCD-scale uncertainties (in percentage) are shown.

state	σ_{LO} [fb]	f_{LO} [%]	σ_{NLO} [fb]	f_{NLO} [%]	K_{NLO}	$K_{\text{NLO}}^{(\text{no g})}$
resolved setup, $Z(e^+e^-)W^+(\text{jj})$						
unpol.	1.8567(2) $^{+1.2\%}_{-1.4\%}$	100	3.036(2) $^{+6.8\%}_{-5.3\%}$	100	1.635	1.033
$Z_L W_L^+$	0.64603(5) $^{+0.2\%}_{-0.6\%}$	34.8	0.6127(4) $^{+0.9\%}_{-0.7\%}$	20.2	0.948	1.031
$Z_L W_T^+$	0.08687(1) $^{+0.2\%}_{-0.6\%}$	4.7	0.17012(6) $^{+8.6\%}_{-6.8\%}$	5.6	1.958	0.967
$Z_T W_L^+$	0.08710(1) $^{+0.1\%}_{-0.6\%}$	4.7	0.24307(7) $^{+10.2\%}_{-8.2\%}$	8.0	2.791	1.017
$Z_T W_T^+$	0.97678(7) $^{+2.0\%}_{-2.2\%}$	52.6	2.0008(7) $^{+8.9\%}_{-7.1\%}$	65.8	2.048	1.059
interf.	0.0595(1)	3.2	0.009(2)	0.4	–	–
unresolved setup, $Z(e^+e^-)W^+(\text{J})$						
unpol.	1.6879(2) $^{+1.9\%}_{-2.1\%}$	100	3.112(2) $^{+7.6\%}_{-6.1\%}$	100	1.843	1.193
$Z_L W_L^+$	0.61653(5) $^{+1.0\%}_{-1.3\%}$	36.5	0.6799(5) $^{+0.9\%}_{-0.7\%}$	21.9	1.103	1.170
$Z_L W_T^+$	0.06444(1) $^{+0.7\%}_{-1.0\%}$	3.8	0.17584(6) $^{+10.8\%}_{-8.6\%}$	5.7	2.729	1.158
$Z_T W_L^+$	0.07437(1) $^{+0.6\%}_{-0.9\%}$	4.4	0.24742(8) $^{+11.0\%}_{-8.9\%}$	8.0	3.327	1.193
$Z_T W_T^+$	0.88233(9) $^{+2.9\%}_{-2.9\%}$	52.3	2.0041(8) $^{+9.6\%}_{-7.7\%}$	64.3	2.271	1.227
interf.	0.0503(3)	3.0	0.004(2)	0.1	–	–

3 Polarised di-boson production with semi-leptonic decays

Very recently, the first calculation of di-boson inclusive production in the semi-leptonic decay channel has been carried out at NLO QCD in the presence of polarised bosons¹². This was done in the MOCANLO Monte Carlo code with tree-level and one-loop SM amplitudes calculated with RECOLA¹³ and COLLIER¹⁴ libraries. The considered process is $pp \rightarrow Z(\rightarrow e^+e^-)W^+(\rightarrow \text{jets})$ at $\sqrt{s} = 13.6\text{TeV}$, with fiducial selections that mimic those of a recent CMS analysis¹⁵. Two setups are studied, depending on the two-light-jet (resolved) or one-fat-jet (unresolved) hadronic decay of the W boson. A boosted regime for both bosons is considered ($p_{\text{T},V} > 200\text{GeV}$). Polarisation states (L=longitudinal, T=transverse) are defined in the centre-of-mass frame of the di-boson system. The integrated cross sections are shown in Table 1. The large NLO QCD corrections mostly come from gluon-initiated real contributions. A large LL fraction characterises the boosted regime, compared to inclusive setups. The longitudinal state is unsuppressed, due to the presence of the triple-gauge coupling. Sizeable differences are found between the two setups at LO, owing to jet recombination, while they become smaller at NLO. Interference contributions are very small, especially at NLO (less than 0.5% of the total).

It is essential to study the differential distributions for (doubly) polarised signals, which typically feature an enhanced discrimination power between longitudinal and transverse states. In Fig. 2 the transverse momentum of the positron is considered for the two setups and for the various polarisation states. There is a clear sensitivity to the Z-boson polarisation in the low-transverse-momentum range. The faster decrease of the curves in the high- p_{T,e^+} regime at LO in the resolved setup gives larger K -factors than in the unresolved setup. A number of other observables have very strong discrimination power amongst the doubly polarised states¹².

4 Conclusions

The extraction of polarised-boson signals is of high interest for the LHC community, with ongoing (and upcoming) data analyses triggering new phenomenological studies and theoretical developments. So far most of the theoretical effort has been devoted to SM fixed-order predictions (QCD and EW corrections), to the automation in Monte Carlo codes, and to the search for polarisation-sensitive observables, with special focus on di-boson production. The calculation of polarised predictions matched to parton-shower is ongoing. In the coming years, it will be desirable to achieve accurate SM predictions for polarised vector-boson scattering (the *golden channel* for polarisation) and to study new-physics effects in the production and the decay of

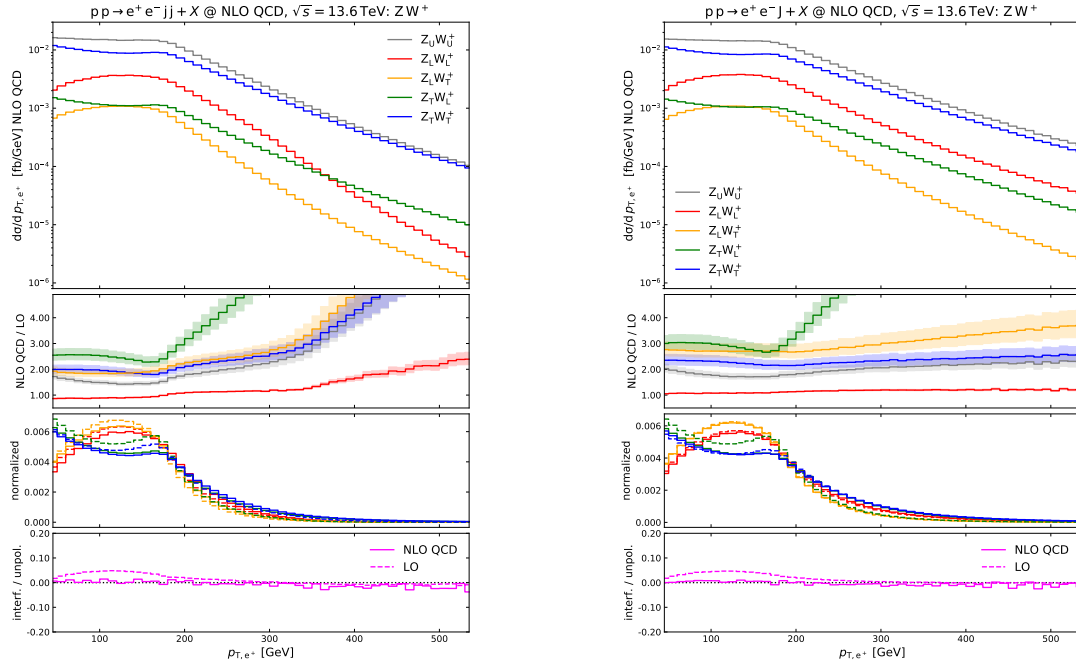


Figure 2 – Distributions in the positron transverse momentum for polarised and unpolarised ZW^+ production in the semi-leptonic decay channel, for the resolved (left) and unresolved (right) setups. From top down: differential cross sections, NLO QCD K -factors, normalised distributions (unit integral), relative interference contribution.

polarised bosons.

References

1. G. Aad *et al.*, Eur. Phys. J. C **72** (2012), 200; S. Chatrchyan *et al.*, Phys. Rev. Lett. **107** (2011), 021802; A. M. Sirunyan *et al.*, Phys. Rev. D **102** (2020) no.9, 092012; V. Khachatryan *et al.*, Phys. Lett. B **750** (2015), 154-175; G. Aad *et al.*, JHEP **08** (2016), 159; V. Khachatryan *et al.*, Phys. Lett. B **762** (2016), 512-534; M. Aaboud *et al.*, Eur. Phys. J. C **77** (2017) no.4, 264; G. Aad *et al.*, JHEP **08** (2020) no.08, 051
2. M. Aaboud *et al.*, Eur. Phys. J. C **79** (2019) no.6, 535 A. Tumasyan *et al.*, JHEP **07** (2022), 032, arXiv:2211.09435 [hep-ex]
3. A. M. Sirunyan *et al.*, Phys. Lett. B **812** (2021), 136018
4. P. Azzi, *et al.* CERN Yellow Rep. Monogr. **7** (2019), 1-220 J. Roloff *et al.* Phys. Rev. D **104** (2021) no.9, 093002
5. Z. Bern *et al.* Phys. Rev. D **84** (2011), 034008; W. J. Stirling and E. Vryonidou, JHEP **07** (2012), 124
6. A. Ballestrero, E. Maina and G. Pelliccioli, JHEP **03** (2018), 170
7. P. Artoisenet *et al.* JHEP **03** (2013), 015; A. Denner *et al.* Nucl. Phys. B **587** (2000), 67-117
8. A. Denner and G. Pelliccioli, JHEP **09** (2020), 164; JHEP **10** (2021), 097
9. D. N. Le and J. Baglio, Eur. Phys. J. C **82** (2022) no.10, 917
10. R. Poncelet and A. Popescu, JHEP **07** (2021), 023
11. T. Ježo and P. Nason, JHEP **12** (2015), 065; G. Pelliccioli, G. Zanderighi, in preparation
12. A. Denner, C. Haitz and G. Pelliccioli, Phys. Rev. D **107** (2023) no.5, 053004
13. S. Actis *et al.*, Comput. Phys. Commun. **214** (2017), 140-173
14. A. Denner, S. Dittmaier and L. Hofer, Comput. Phys. Commun. **212** (2017), 220-238
15. A. Tumasyan *et al.*, JHEP **04** (2022), 087